Supplemental Material

Proteomic and functional studies reveal detyrosinated tubulin as treatment target in sarcomere mutation-induced hypertrophic cardiomyopathy

Authors:

Maike Schuldt[1], MSc, Jiayi Pei[2], MSc, Magdalena Harakalova[2], PhD, Larissa M. Dorsch[1], MSc, Saskia Schlossarek[3,4], PhD, Michal Mokry[5], PhD, Jaco C. Knol[6], PhD, Thang V. Pham[6], PhD, Tim Schelfhorst[6], BSc, Sander R. Piersma[6], PhD, Cris dos Remedios[7], PhD, Michiel Dalinghaus[8], MD, PhD, Michelle Michels[9], MD, PhD, Folkert W. Asselbergs[2,10,11], MD, PhD, Marie-Jo Moutin[12], PhD, Lucie Carrier[3,4], PhD, Connie R. Jimenez[6], PhD, Jolanda van der Velden[1‡]*, PhD, Diederik W.D. Kuster[1‡]*, PhD

[‡]shared last author

*corresponding author

Affiliations:

[1]Amsterdam UMC, Vrije Universiteit Amsterdam, Department of Physiology, Amsterdam Cardiovascular Sciences, Amsterdam, The Netherlands

[2]Department of Cardiology, Division Heart and Lungs, University Medical Center Utrecht, Utrecht, The Netherlands

[3]Institute of Experimental Pharmacology and Toxicology, Cardiovascular Research Center, University Medical Center Hamburg-Eppendorf, Hamburg, Germany

[4]DZHK (German Centre for Cardiovascular Research), partner site Hamburg/Kiel/Lübeck, Hamburg, Germany

[5]Department of Pediatric Gastroenterology, Wilhelmina Children's Hospital, University Medical Center Utrecht, Utrecht, The Netherlands

[6]Amsterdam UMC, Vrije Universiteit Amsterdam, Department of Medical Oncology, OncoProteomics Laboratory, VUmc-Cancer Center Amsterdam, Amsterdam, The Netherlands

[7]Sydney Heart Bank, Discipline of Anatomy, Bosch Institute, University of Sydney, Sydney, Australia

[8]Department of Pediatric Cardiology, Erasmus Medical Center Rotterdam, Rotterdam, The Netherlands

[9]Department of Cardiology, Thorax Center, Erasmus Medical Center Rotterdam, Rotterdam, The Netherlands

[10]Institute of Cardiovascular Science, Faculty of Population Health Sciences, University College London, London, United Kingdom

[11]Health Data Research UK and Institute of Health Informatics, University College London, London, United Kingdom

[12]Grenoble Institut des Neurosciences (GIN), Université Grenoble Alpes, Grenoble, France

Supplemental Methods

Proteomics analysis

In-gel digestion

In-gel digestion was performed as described previously[16]. The proteins were in-gel reduced with 10 mM DTT and alkylated with 54 mM iodoacetamide. Each gel lane was cut into 5 pieces (*Figure S1*) which were subsequently sliced into 1 mm^3 cubes. Proteins were digested in-gel with 6.3 ng/ml trypsin. Peptides were extracted from gel slices with 1% formic acid and 5% formic acid/50% acetonitrile and concentrated in a vacuum centrifuge prior to nano-LC-MS/MS measurement. Samples were measured by LC-MS per gel band starting at the high molecular weight (MW) fraction for all samples, before continuing with the next gel band until the last (low MW fraction) band was measured. Injections alternated between all different group samples to minimize experimental bias between groups.

Nano-LC-MS/MS

Analysis of the experiment was performed as described in Piersma et al[17]. Peptides were separated using an Ultimate 3000 Nano LC-MS/MS system (Dionex LC-Packings, Amsterdam, The Netherlands) equipped with a 40 cm x 75 µm ID fused silica column custom packed with 1.9 µm ,120 Å ReproSil Pur C18 aqua (Dr Maisch GMBH, Ammerbuch-Entringen, Germany). After injection, peptides were trapped at 6 µl/min on a 10 mm × 100 µm ID trap column packed with 5 µm, 120 Å ReproSil Pur C18aqua at 2% buffer B (buffer A: 0.5% acetic acid (Fischer Scientific), buffer B: 80% acetonitrile, 0.5% acetic acid) and separated at 300 nl/min in a 10–40% buffer B gradient in 60 minutes (90 min inject-to-inject). Eluting peptides were ionized at a potential of + 2 kV into a Q Exactive mass spectrometer (Thermo Fisher, Bremen, Germany). Intact masses were measured at resolution 70,000 (at m/z 200) in the orbitrap using an automatic gain control (AGC) target value of $3x10^6$ charges. The top 10 peptide signals (charge-states 2+ and higher) were submitted to MS/MS in the HCD (higher-energy collision) cell using 1.6 amu isolation width and 25% normalized collision energy. MS/MS spectra were acquired at resolution 17,500 (at m/z 200) in the orbitrap using an AGC target value of $1x10^6$ charges, a maxIT of 60 ms and an underfill ratio of 0.1%. Dynamic exclusion was applied with a repeat count of 1 and an exclusion time of 30 s.

Data analysis

MS/MS spectra were searched against a Uniprot human reference proteome FASTA file (Swissprot_2017_03_human_canonical_and_isoform.fasta, 42161 entries) using MaxQuant version 1.5.4.1. Enzyme specificity was set to trypsin and up to two missed cleavages were allowed. Cysteine

carboxamidomethylation was treated as fixed modification, and methionine oxidation and N-terminal acetylation as variable modifications. Peptide precursor ions were searched with a maximum mass deviation of 4.5 parts per million (ppm) and fragment ions with a maximum mass deviation of 20 ppm. Peptide and protein identifications were filtered at a false discovery rate (FDR) of 1% using the decoy database strategy. The minimal peptide length was 7 amino acids, the minimum Andromeda score for modified peptides was 40, and the minimum delta score was 6. Proteins that could not be differentiated based on MS/MS spectra alone were grouped to protein groups (default MaxQuant settings). Searches were performed with the label-free quantification option selected.

RNA sequencing (RNAseq)

RNA was isolated using ISOLATE II RNA Mini Kit (Bioline) according to the manufacturer's instructions with minor adjustments (10 min digestion using 20 µg proteinase K and a subsequent washing step using 100% ethanol were added after the lysis step). Sample quality and quantity was assessed using the 2100 Bioanalyzer with a RNA 6000 Pico Kit (Agilent), and Qubit Flourometer with a HS RNA Assay (Thermo Fisher). After selecting the polyadenylated fraction of RNA, libraries were prepared using the NEXTflexTM Rapid RNA-seq Kit (Bioo Scientific). Libraries were sequenced on the Nextseq500 Illumina platform, producing 75 bp long single end reads. Reads were aligned to the human reference genome GRCh37 using STAR v2.4.2a[60]. Picard's AddOrReplaceReadGroups v1.98 (http://broadinstitute.github.io/picard/) was used to add read groups to the BAM files, which were sorted with Sambamba v0.4.5[61] and transcript abundances were quantified with HTSeq-count v0.6.1p1[62] using the union mode. Subsequently, reads per kilobase million reads sequenced (RPKMs) were calculated with edgeR's RPKM function[63]. In order to obtain a list of differentially expressed genes between HCM and controls at false discovery rate (FDR) <0.05, we employed Deseq2 using Galaxy[64, 65]. The calculated p-values were calculated using Wald statistics and corrected for multiple testing using the Benjamini-Hochberg method. Statistics of the sequencing results can be found in *Table S6*. *Table S5* lists the RNA expression data of the genes that we detected at the protein level.

We applied Gene Set Enrichment Analysis[66] to examine the correlation between the proteomics data and the transcriptome profile revealed by RNA-seq. Briefly, differentially expressed genes (p-value <0.05) were included and ranked according to their fold change. The correlation between differentially regulated proteins and differentially expressed genes was assessed with the standard settings.

Generation of the MYBPC3$_{2373insG}$ mouse model

The *MYBPC3*$_{2373insG}$ mouse model was engineered using CRISPR/Cas9[67]. CRISPR guide RNAs, used for mouse Mybpc3 gene knock-in were designed using CRISPR.mit.edu. T guides were selected and produced by PCR using as the template Addgene pX330 plasmid (pX330-U6-Chimeric_BB-CBh-

hSpCas9), carrying the scaffold portion of the guide. The forward primer consisted of a T7 promoter sequence and target sequence. A single guide RNA (sgRNA) was designed to target the following sequence in the *mybpc3* gene: GGACTCCTGCACTGTGCAGT*GGG* (PAM sequence in italic). sgRNA was made by in vitro transcription using Ambion's MEGAshortscript kit, and later purified with a MEGAclear kit. Commercial Cas9 mRNA was ordered from TriLink (L-6125, USA) and used for the embryo microinjection. Cas9 protein was ordered from PNA Bio (CP01-50, USA) and used to check cutting efficiency of the guides in vitro. Single strand donor oligonucleotides (ssODNs) with 60-80 bp homology to sequences on each side of the gRNA-mediated double-stranded break were designed and ordered from IDT. A silent mutation introducing RsaI restriction site in the oligo was created for genotyping purposes. Fertilized eggs were collected from the oviducts of super ovulated BL6/J females. Microinjection was performed by continuous flow injection of the Cas9/gRNA/ssODN mixture into the cytoplasm of 1-cell zygotes using the following final concentrations 100/50/200 ng/ul, respectively. Tail-tipping of the newborn mice was utilized to purify DNA for genotyping by PCR, employing two screening primers: forward, 5'- GTAAGGTAATCCGGGTCTAGATAGC and reverse, 5'- ACTCGCATCTCATAGGCTACACC, producing 433bp band for the WT and two additional bands of 179bp and 254bp in the positive mice when restricted with RsaI.

Measurement of calcium transients in intact MYBPC3$_{2373insG}$ cardiomyocytes

In a subset of cardiomyocytes calcium transient measurements were performed. Cardiomyocytes were loaded with 1µM fura-2AM in culture medium for 15 minutes. After this cells were washed twice with tyrode solution. Calcium transients were measured after 30 minutes to allow for complete de-esterification. Calcium transients were recorded on the Ionoptix/CytoCypher MultiCell system (CytoCypher BV, the Netherlands) with a dual-excitation fluorescence photomultiplier system (IonOptix, Westwood, Massachusetts). A single cell was excited by rapidly switching between a 340nm and 385nm LED light source, fluorescence emission was then detected between 480-510nm and analyzed using CytoSolver software (CytoCypher BV, the Netherlands). An R^2 >0.8 for peak fit and >0.9 for recovery fit as well as a signal to noise ratio >5 was selected as inclusion criteria for calcium data. Because fura loading might influence contraction by buffering Ca^{2+}, we used cells that were not loaded for fura-2AM for the contractility measurements.

Protein analysis

For protein expression analysis by Western blot tissue lysates (whole tissue lysate for human and *MYBPC3*$_{2373insG}$ mice; cytosolic fraction lysate for *MYBPC3*$_{772G>A}$ mice) were prepared and proteins separated on a precast Bio-Rad Criterion TGX-gel and transferred to a polyvinylidene difluoride membrane. Site-specific antibodies directed to ERK (Cell Signaling, 9102S), phospho-ERK (Cell

Signaling, 4370S), AKT (Cell Signaling, 9272S), phospho-Ser473-AKT (Cell Signaling, 4060S), α-tubulin (Sigma, T9026), tyrosinated tubulin (Sigma, T9028), detyrosinated tubulin (abcam, ab48389), desmin (Cell Signaling, 5332S) and GAPDH (Cell Signaling, 2118S; HyTest, 5G4 for *MYBPC3*$_{772G>A}$ mice) were used to detect the proteins which were visualized with an enhanced chemiluminescence detection kit (Amersham) and scanned with Amersham Imager 600 or with LI-COR near-infrared detection system. In the specific case of *MYBPC3*$_{772G>A}$ mice, antibodies directed against total- (clone α-3A1), detyrosinated- (clone J63) and tyrosinated- (clone YL1/2) α-tubulin were generously provided by Marie-Jo Moutin (Grenoble, France)[56]. Protein expression was determined by densitometric analysis. Protein expression was normalized to GAPDH or the total protein in case of phosphorylation-specific antibodies or total protein stain (TPS) with the LI-COR system.

Statistics

Graphpad Prism v7 software was used for statistical analysis. Data (except proteomics and RNAseq data) were statistically analyzed with the Student's *t*-test when comparing 2 groups or 2way ANOVA with Tukey's multiple comparisons test when comparing more than one group. Data that did not pass the D'Agostino & Pearson normality test were analyzed with the non-parametric Mann-Whitney test when comparing two groups and Kruskal-Wallis test with Dunn's multiple comparisons test when comparing more than 2 groups. All values are shown as means ± standard errors of the mean. Patient characteristics are reported as mean ± standard deviation or median with interquartile range when appropriate. Categorical distributions are presented as frequencies and statistically analyzed with Fisher's exact test. A p-value ≤0.05 was considered as significantly different.

Supplemental Tables

Table S1: Patient characteristics[#]. Dark grey row below each group shows mean±SD per group.

Group	HCM ID	Sex	Age at surgery (yrs)	Mutation code	type	LV parameters: LAD (mm)	IVS (mm)	IVS_i	EDD (mm)	ESD (mm)	FS (%)	Diastolic parameters: E/A ratio	E/e' ratio	TR velocity (cm/s)	Diastolic dysfunction stage (1-4)	Systolic parameters: LVOTO (mmHg)	Medication
MYBPC3$_{2373insG}$	42	M	32	MYBPC3 c.2373insG/p.W792fs	trunc	47	23	13	43	16	63	1.03	14.20		2	64	bb, ccb
	43	M	60	MYBPC3 c.2373insG/p.W792fs	trunc	52	23		45	29	36	2.00	14.50		3	77	bb, ccb
	83	M	17	MYBPC3 c.2373insG/p.W792fs	trunc												
	103	M	26	MYBPC3 c.2373insG/p.W792fs	trunc	47	20	9	47	25	47	1.33	13.80	1.40	1	13	bb, snri
	104	M	33	MYBPC3 c.2373insG/p.W792fs	trunc	33	24	13	40	25	38	1.08	8.90	no	1	31	bb
	120	M	27	MYBPC3 c.2373insG/p.W792fs	trunc	39	24	13	37	19	49	1.42	14.00	2.33	1	61	bb
	123	F	59	MYBPC3 c.2373insG/p.W792fs	trunc	45	21		55			1.20	32.90	3.12	2	64	bb, ccb, oac, diuretics, ACEi
	159	M	40	MYBPC3 c.2373insG/p.W792fs	trunc	48	24	11	34	23	32	1.00	17.90	2.47	1	85	bb
	169	M	52	MYBPC3 c.2373insG/p.W792fs	trunc	45	21	10	43			0.87	15.90	2.27	1	100	bb, ccb, haldol, vpa
		89% male	38±15			45±6	23±2	12±2	43±6	23±5	44±11	1.24±0.36	16.51±7.09	2.32±0.61	2±1	62±28	
MYBPC3$_{other}$	34	F	47	MYBPC3 c.1790G>A/p.R597Q	trunc	46	20	10	42	18	57	2.00	18.30	2.99	3	38	bb, ccb, statin
	36	M	22	MYBPC3 c.927-2A>G	trunc	60	30		44	19	57	0.73	16.00	no	1	71	bb, ccb
	47	M	55	MYBPC3 c.3407_3409del/p.Y1136del	del		25	13	40			1.57	21.00	2.88	2	96	ccb
	52	F	24	MYBPC3 c.2827C>T/p.R943X	trunc	44	24	14	35	16	54	1.12	18.90	2.50	2	34	bb
	62	M	36	MYBPC3 c.772G>A/p.E258K	trunc	37	27	14	32	18	44	1.21	10.80	1.80	1	3	bb, diuretics, ACEi
	63	M	33	MYBPC3 c.2827C>T/p.R943X	trunc	40	21	12	46	20	57	2.38	19.50	no	3	25	bb, ccb
	71	M	49	MYBPC3 c.2827C>T/p.R943X	trunc	47	16	7	44	29	34	0.78	10.20	2.30	1	9	bb
	113	F	21	MYBPC3 c.2434G>A,c.2827C>T/p.R943X	trunc	43	45	28	40			1.26	23.10	2.29	2	27	bb, ccb

	116	F	53	MYBPC3 c.2827C>T/p.R943X	trunc											
	124	M	53	MYBPC3 c.2827C>T/p.R943X	trunc	43	21	10	47			0.64	13.50	2.15	1	41	bb
	133	M	58	MYBPC3 c.442G>A/p.G148R	mis	44	21	10	40	30	25	0.86	12.50	2.42	1	19	bb, oac, statin, ppi, NaSSA, ssri
		64% male	41±14			45±6	25±8	13±6	41±5	21±6	47±13	1.26±0.58	16.38±4.46	2.42±0.38	2±1	36±28	
MYH7	27	F	58	MYH7 c.4130C>T/p.T1377M	mis	48	20	13						2.80		100	bb
MYH7	42B	F	46	MYH7 c.1816G>A/p.V606M	mis	51	20	9				3.38	20.30	2.60	3	77	bb, ccb
MYH7	80	M	34	MYH7 c.1291G>C/p.V431L	mis		17	8	45			1.45	14.30	1.41	1	85	bb, ccb
MYH7	92	M	66	MYH7 c.2685A>C/p.Q895H	mis												
MYH7	106	M	35	MYH7 c.2783A>T/p.D928V	mis		16	8	47			0.93	11.50	2.06	1	16	bb
MYH7	114	M	69	MYH7 c.976G>C/p.A326P	mis	43	19		33			0.60	12.90	2.14	1	71	bb, statin, asa
MYH7	119	M	41	MYH7 c.3367G>A/p.E1233K	mis	56	20	9				1.26	20.40	1.40	2	81	bb
MYH7	130	M	72	MYH7 c.976G>C/p.A326P	mis	42	18	9	50			2.60	18.60	3.30	3	27	bb, statin, ppi, amiodaron, noac, metformin
MYH7	131	F	52	MYH7 c.1987C>T/p.R663C	mis	52	21	10	43					no		41	bb, statin, asa
MYH7	166	F	66	MYH7 c.2080C>T/p.R694C	mis	41	16					0.79	32.40	no	2	41	bb, ccb, asa, pregabaline
		60% male	54±14			48±6	19±2	10±2	44±6			1.57±1.03	18.63±7.05	2.24±0.71	2±1	60±29	
Other (TNNI3/TNNT2/MYL2)	55	M	46	TNNI3 c.433C>T/p.R145W	mis	64	23	11	42	23	45	1.09	26.70	no	2	100	bb
Other (TNNI3/TNNT2/MYL2)	88	F	57	MYL2 c.401A>C/p.E134A	mis												
Other (TNNI3/TNNT2/MYL2)	132	F	15	TNNT2 c.814C>T/p.Q272*	trunc	37	19	13	39	16	59	2.33	17.50	1.99	3	81	bb
Other (TNNI3/TNNT2/MYL2)	135	M	68	MYL2 c.64G>A/p.E22K	mis	43	16		48			1.20	10.00		2	23	
Other (TNNI3/TNNT2/MYL2)	163	F	64	TNNI3 c.433C>T/p.R145W	mis	46	23	12	42			0.52	16.30	no	1	125	bb, asa, thyroxine
Other (TNNI3/TNNT2/MYL2)	164	M	0.2	MYL2													
Other (TNNI3/TNNT2/MYL2)	170	F	69	TNNI3 c.433C>T/p.R145W	mis	47	22		41			0.78	36.80	2.02	2	36	bb, ccb, oac, ppi, diuretic, pcm
Other (TNNI3/TNNT2/MYL2)	173	M	58	TNNT2 c.832C>T/p.R278C	mis	51	18		40		62	2.04	16.60	2.70	3	74	non
Other (TNNI3/TNNT2/MYL2)	175	M	61	TNNT2 c.832C>T/p.R278C	mis	46	16	8	50			0.75	12.50	2.25	1	31	bb, asa, diuretics, clopidogrel, statin

		56% male	49±25			48±8	20±3	11±2	43±4	20±5	55±9	1.24±0.69	19.49±9.25	2.24±0.33	2±1	67±38	
HCM_{SMN}	40	M	22	SMN (48 genes NGS)		54	15	7	53	28	47		47.30		3	100	ccb
	90	M	53	SMN (48 genes NGS)		41	17	9	46	24	48	1.03				61	bb
	100	M	41	SMN (48 genes NGS)		49	15					0.62	14.80		1	81	bb, ACEi, asa, ppi, gembrofizill, insulin, metformin, nitrate
	105	M	65	SMN (48 genes NGS)		54	16	7				1.10	22.90		2	49	oac, amiodaron, statin
	109	F	71	SMN (48 genes NGS)		52	20	10				1.30	33.60		2	130	bb, asa, ATII-i, ppi, nitrate, statin
	117	F	50	SMN (48 genes NGS)		50	16	10				0.80	24.70		1	159	bb, ccb, asa, ezetrol, calcichew
	125	M	66	SMN (48 genes NGS)		45	18	9	45			2.68	15.20		3	132	bb, oac
	126	F	64	SMN (48 genes NGS)			15	9	34			0.61	17.40		1	104	bb
	156	F	54	SMN (48 genes NGS)		39	15	6	47			0.83	33.30		2	108	bb, ccb, ppi, ACEi, diuretic, ssri
	168	M	46	SMN (48 genes NGS)		49	15	7	41			1.00	20.40		2		ccb, foster, aerius
	172	M	57	SMN (48 genes NGS)			20					0.68	16.20		1	21	ccb, ATII-i, insulin
		64% male	54±14			48±5	17±2	8±1	44±6	26±3	48±1	1.07±0.61	24.58±10.54		2±1	95±42	
NF_{IVS}	5033	F	48														
	5126	F	55														
	6008	M	40														
	6028	F	62														
	6056	F	42														
	7040	M	37														
	7054	M	33														
	8004	F	50														
		38% male	46±10														

[#] The table is showing the exact mutation, including mutation type (missense (mis), truncation (trunc) or deletion (del)), per sample. Furthermore it presents the left ventricular (LV) parameters left atrial diameter (LAD), interventricular septum thickness (IVS), indexed interventricular septum thickness (IVS_i), which is corrected for body surface area, end-diastolic diameter (EDD), end-systolic diameter (ESD) and fractional shortening (FS) as well as the diastolic parameters E/A ratio, E/e‘ ratio and TR velocity. The table also displays the stage of diastolic dysfunction, the systolic left ventricular outflow tract obstruction gradient (LVOTO) and information about the patient’s medication (beta-blocker (bb), calcium channel blocker (ccb), serotonin-norepinephrine reuptake inhibitor (snri), oral anti-coagulant (oac), diuretics, angiotensin-converting enzyme inhibitor (ACEi), valproic acid (vpa), proton pump inhibitor (ppi), noradrenergic and specific serotonergic antidepressant (NaSSA), selective serotonin reuptake inhibitor (ssri), acetylsalicylic acid (asa), non-vitamin k oral anticoagulant (noac), paracetamol (pcm), angiotensin-II receptor inhibitor (ATII-i), next-generation sequencing (NGS).

Table S2: Descriptive matrix of the different group comparisons.

Total n proteins identified		3811		
Total n proteins after filtering		2127		
Group comparison		**n proteins (p<0.05)**		
		total	**upregulated**	**downregulated**
$MYBPC3_{2373insG}$	NF_{IVS}	340	138	202
$MYBPC3_{other}$	NF_{IVS}	480	190	290
MYH7	NF_{IVS}	402	137	265
HCM_{SMN}	NF_{IVS}	381	128	253
Other	NF_{IVS}	336	160	176
HCM_{SMP}	HCM_{SMN}	44	36	11
HCM_{SMP}	NF_{IVS}	511	189	322
HCM_{all}	NF_{IVS}	529	187	342

Table S3: Expression of expected deregulated proteins in HCM patient tissue.

Category	Protein description	Gene symbol	Mean normalized count		Fold change	p value
			NF_{IVS}	HCM_{all}		
ECM	Fibronectin 1	FN1	29.2	46.0	1.57	0.0183
ECM	Thrombospondin-4	THBS4	7.4	31.9	4.33	<0.0001
ECM	Periostin	POSTN	6.8	141.3	20.91	<0.0001
Hypertrophy	Four and a half LIM domains protein 2	FHL2	178.6	136.7	-1.31	0.0006
Hypertrophy	Myosin heavy chain 6	MYH6	124.6	52.2	-2.39	<0.0001
Hypertrophy	Cysteine and glycine-rich protein 3	CSRP3	81.0	97.2	1.20	0.0008

Table S4: Expression of MYBPC3 in the *MYBPC3*$_{2373insG}$ patient group.

Category	Protein description	Gene symbol	Mean normalized count		Fold change	p value
			NF_{IVS}	$MYBPC3_{2373insG}$		
Myofilament	Myosin-binding protein C, cardiac-type	MYBPC3	760.3	639.6	-1.19	0.0005

Table S6: Statistics of RNA sequencing results.

Group	Sample ID	Run	Total number of reads	Number of gene with at least 1 read	Number of genes with at least 10 reads	Percentage of mRNA bases
SMP	HCM104	2	12554384	12095	9990	21,67%
SMP	HCM120	2	13988528	6676	5402	8,18%
SMP	HCM124	3	15375893	14775	10774	16,09%
SMP	HCM130	2	16267099	12720	8466	6,92%
SMP	HCM133	1	14473822	13297	9383	12,96%
SMP	HCM159	3	15262767	14176	10027	13,32%
SMP	HCM163	1	20784562	14387	12646	23,67%
SMP	HCM166	2	11685010	6423	5187	9,24%
SMP	HCM169	3	15482131	13476	9686	14,93%
SMP	HCM173	3	13933213	13989	9134	12,53%
SMP	HCM175	1	19231230	17365	13168	44,63%
SMP	HCM27	1	23603136	16725	12428	30,91%
SMP	HCM42B	3	15751613	14994	10733	20,92%
SMP	HCM43	1	19091911	17260	13007	32,96%
SMP	HCM52	2	28426211	9836	8213	8,71%
SMP	HCM55	1	43944540	18687	14354	33,11%
SMP	HCM62	2	17435209	9500	7648	10,04%
SMP	HCM63	3	9504043	13846	9756	19,79%
SMP	HCM71	3	18548295	14758	10745	13,89%
SMP	HCM80	1	24403651	16984	12850	26,25%

SMP	HCM88	3	24393084	15553	11568	14,50%
SMP	HCM92	1	19953132	17122	13012	29,97%
SMN	HCM105	1	19936992	17150	13224	44,38%
SMN	HCM126	2	11706747	13841	9213	11,93%
SMN	HCM156	2	17999842	14374	10143	11,22%
SMN	HCM168	3	15980714	14325	9753	14,42%
SMN	HCM172	3	15979548	14596	10788	17,21%
SMN	HCM40	1	23610820	16624	12612	30,24%
SMN	HCM90	1	22301135	17517	13330	34,55%
NF	D6056IVS	2	19127904	12675	9379	9,34%
NF	D7054IVS	2	13978089	14115	9978	12,60%
NF	D8004IVS	3	17777029	14827	10542	14,73%
NF	D5033IVS	1	13060130	16222	12191	47,24%
NF	D5126IVS	1	27626362	18097	13637	46,85%

Supplemental Figures

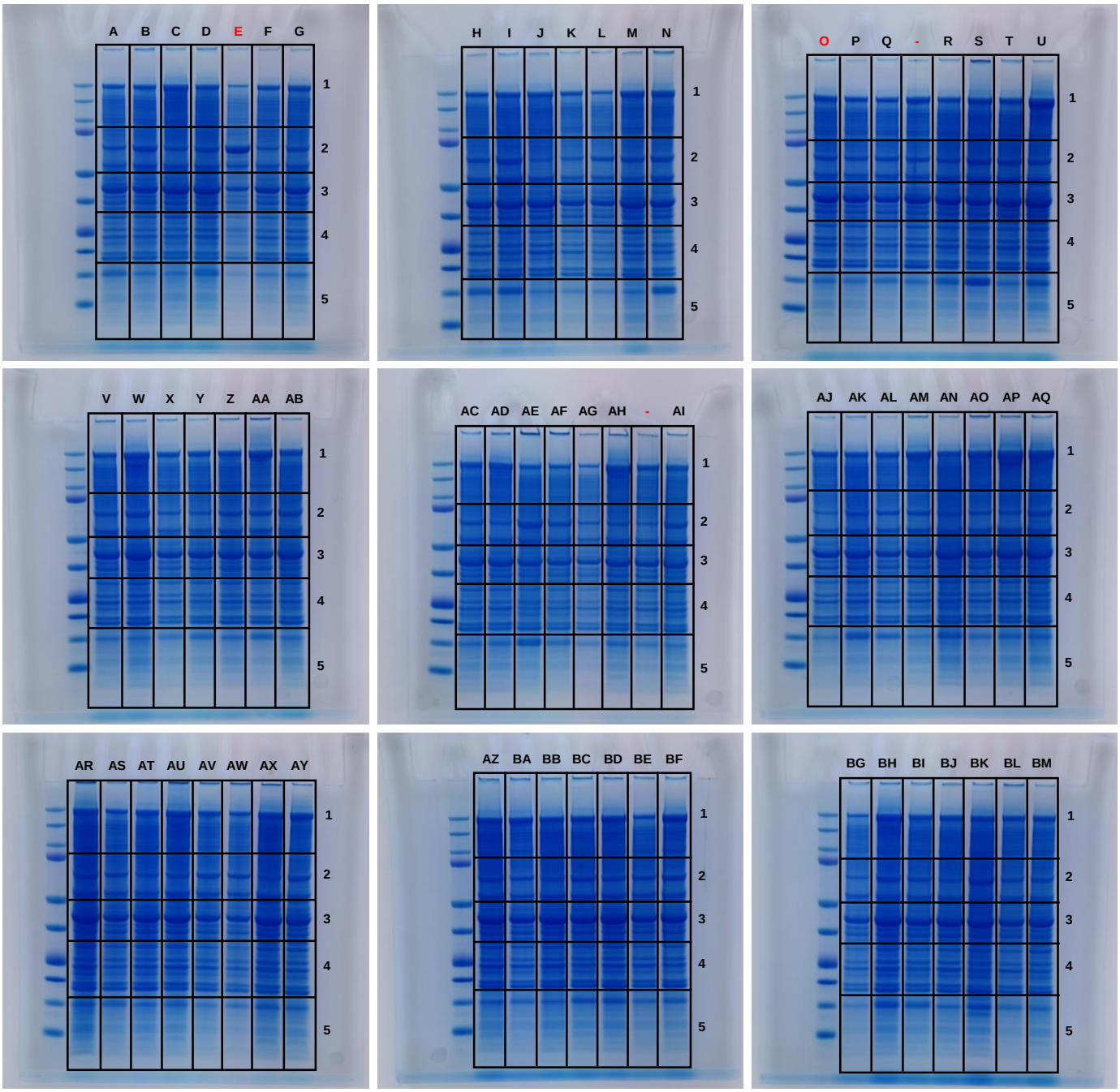

Figure S1: Images of gels that were used for proteomics experiment with slicing scheme. Samples E and O (marked in red) were excluded from analysis.

Figure S2

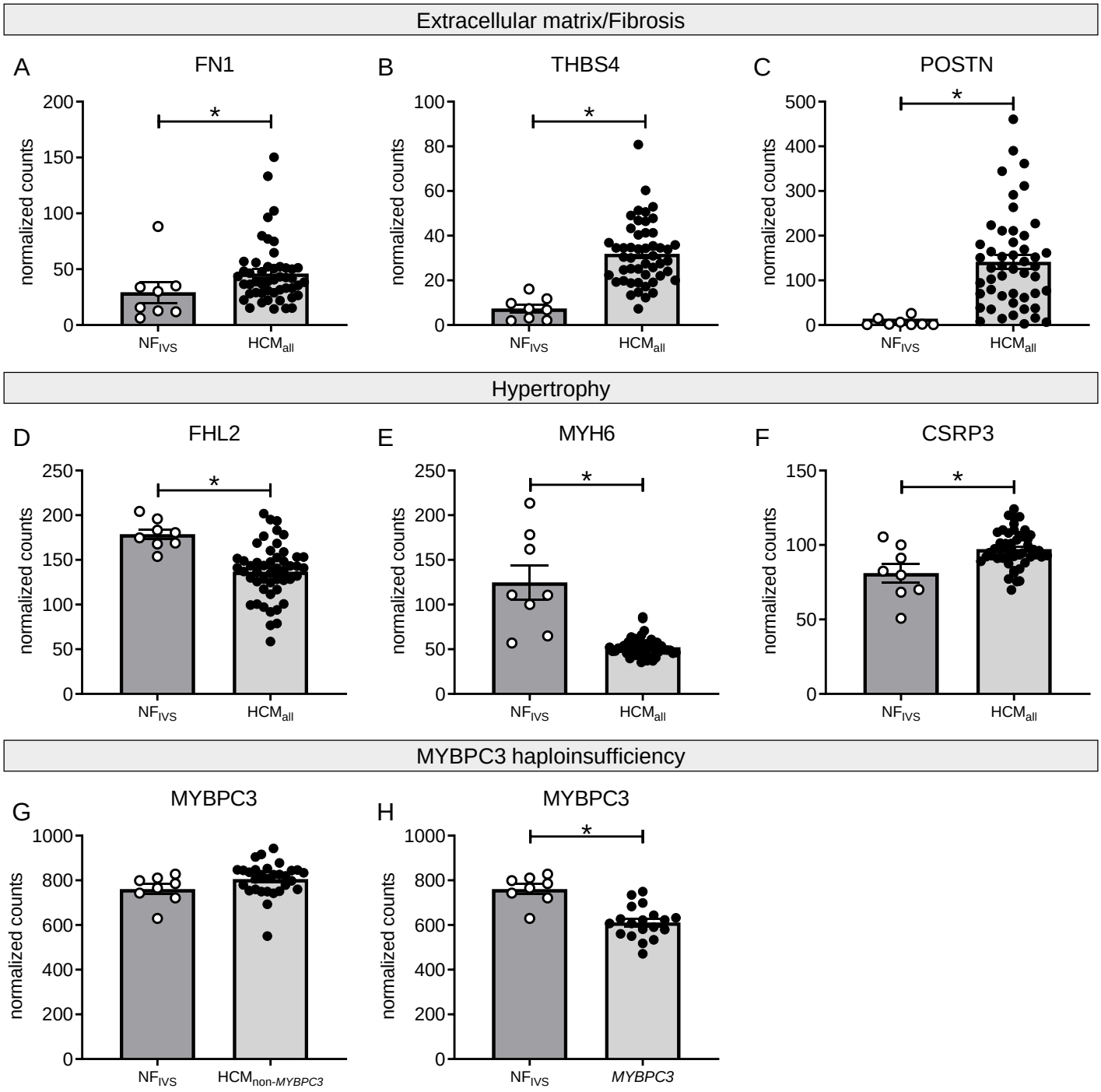

Figure S2: Validation of proteomics analysis with known target proteins. (A-C) show protein expression data of the extracellular matrix proteins FN1, THBS4 and POSTN. (D-F) show protein expression data of the hypertrophy related proteins FHL2, MYH6 and CSRP3. (G) shows expression of MYBPC3 in HCM samples without a mutation in MYBPC3 and (H) with a mutation in MYBPC3. * $p<0.05$ (beta-binomial statistics from the proteomics analysis).

Figure S3

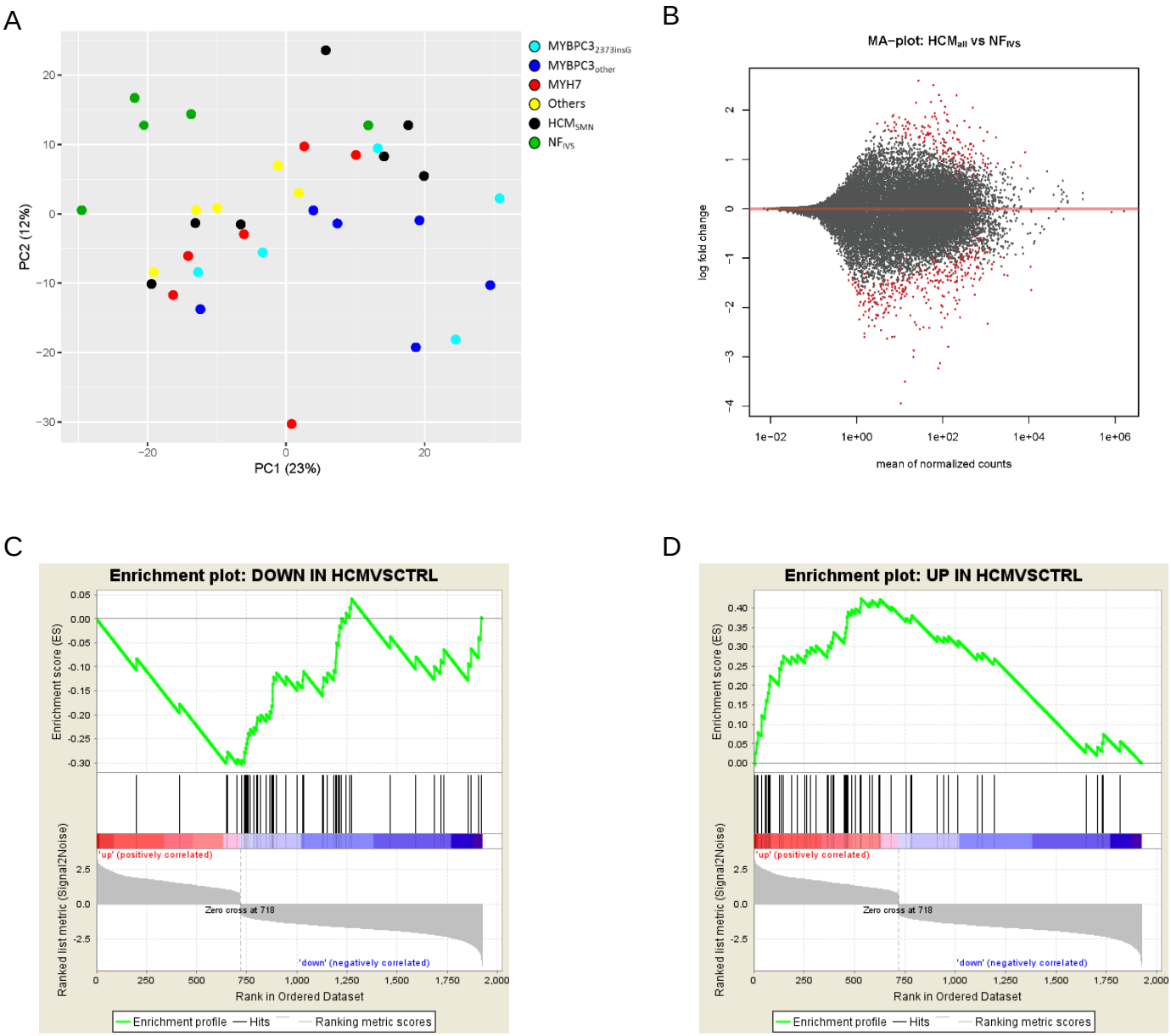

Figure S3: RNA sequencing results. (A) PCA plot of RNA sequencing data shows separate clustering of HCM_{all} and NF_{IVS} samples. (B) MA-plot showing all genes with differentially expressed genes between HCM_{all} and NF_{IVS} depicted in red. Gene set enrichment analysis of downregulated (C) and upregulated (D) proteins and mRNAs shows overall correlation of proteomics and transcriptomics data.

Figure S4

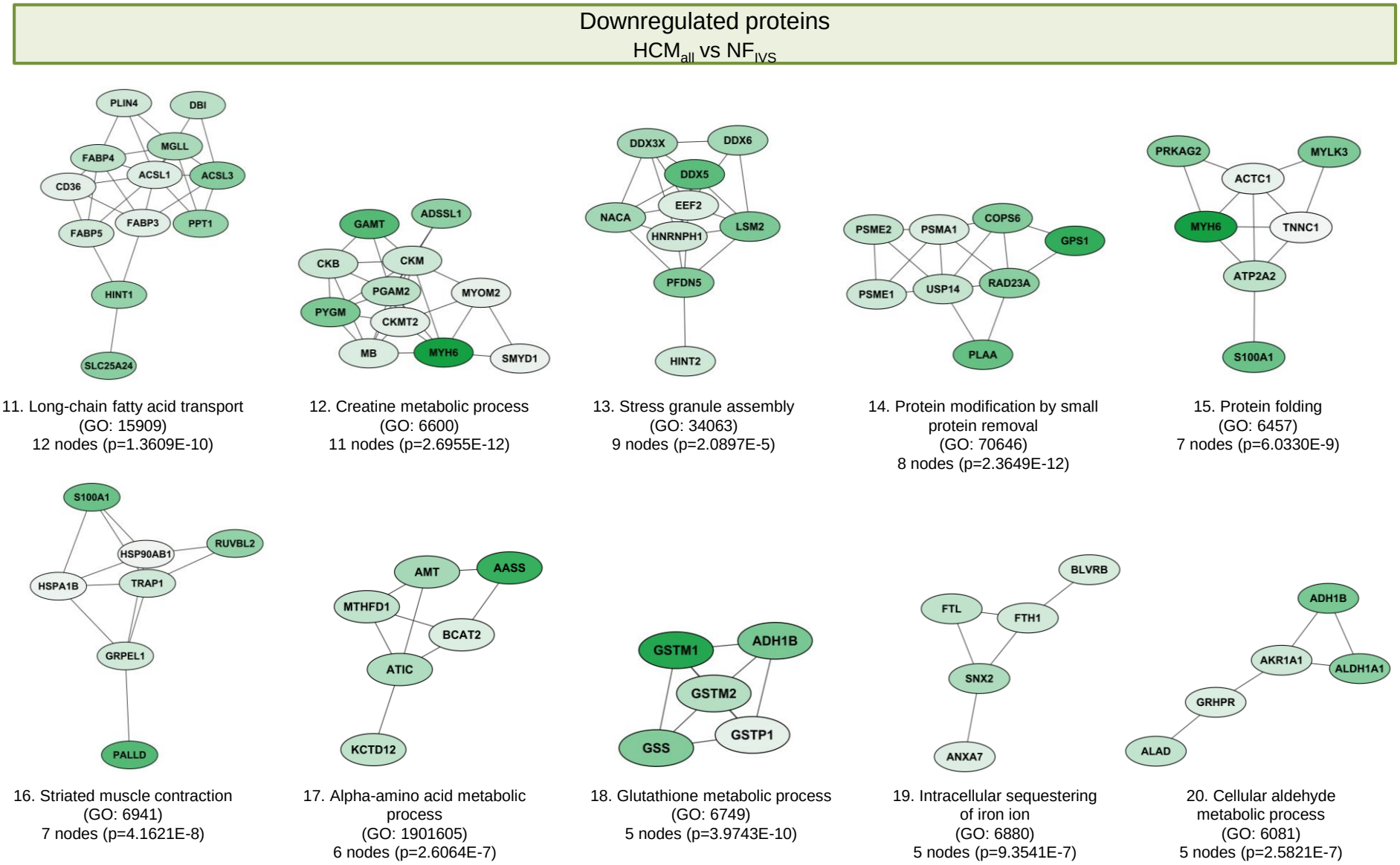

Figure S4: HCM-specific changes in biological processes in downregulated proteins. Extended version of Figure 2A. The color gradient from light to dark indicates an increase in fold change.

Figure S5

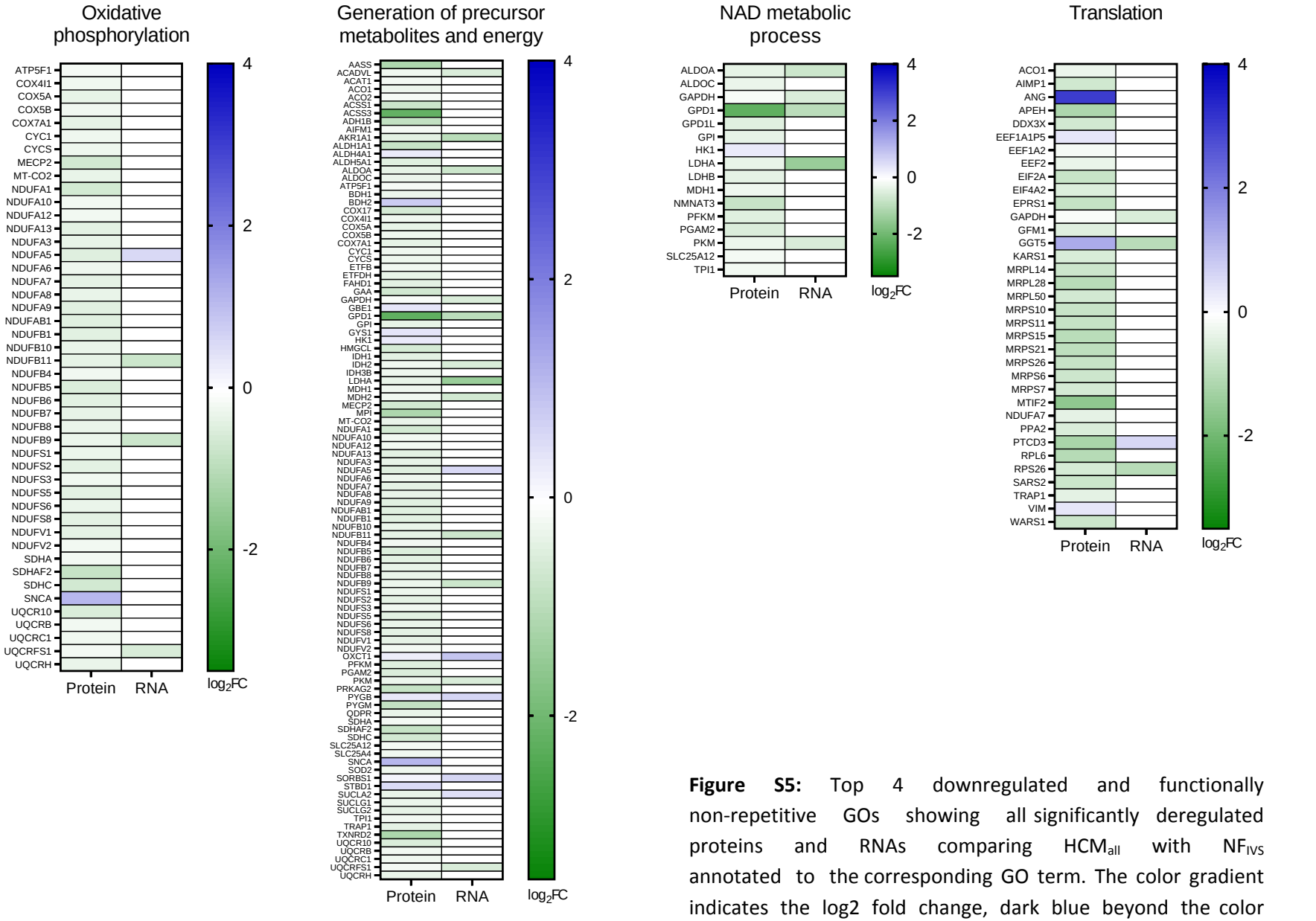

Figure S5: Top 4 downregulated and functionally non-repetitive GOs showing all significantly deregulated proteins and RNAs comparing HCM_{all} with NF_{IVS} annotated to the corresponding GO term. The color gradient indicates the log2 fold change, dark blue beyond the color scale indicates a log2 fold change >4.

Figure S6

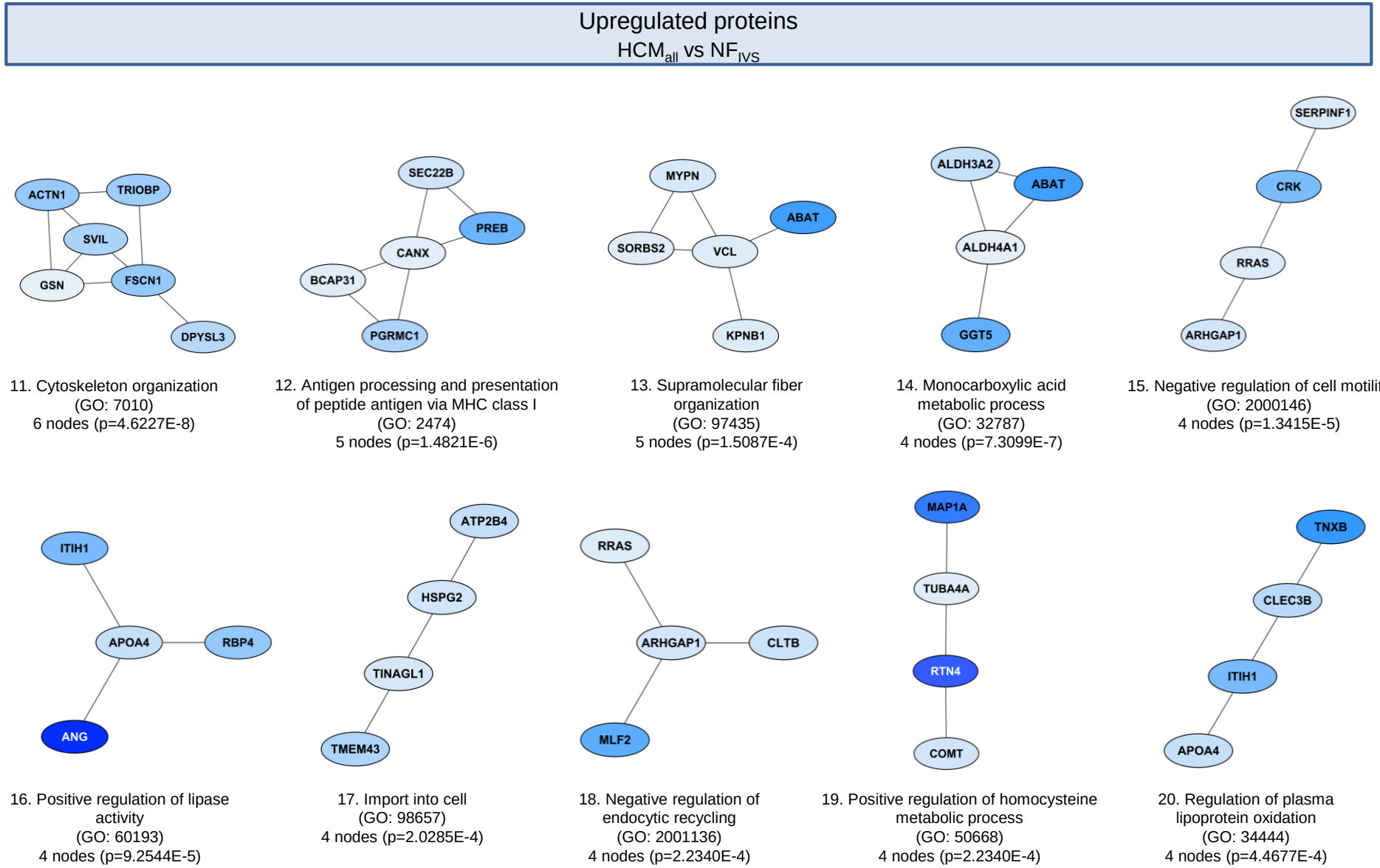

Figure S6: HCM-specific changes in biological processes in upregulated proteins. Extended version of Figure 2B. The color gradient from light to dark indicates an increase in fold change.

Figure S7

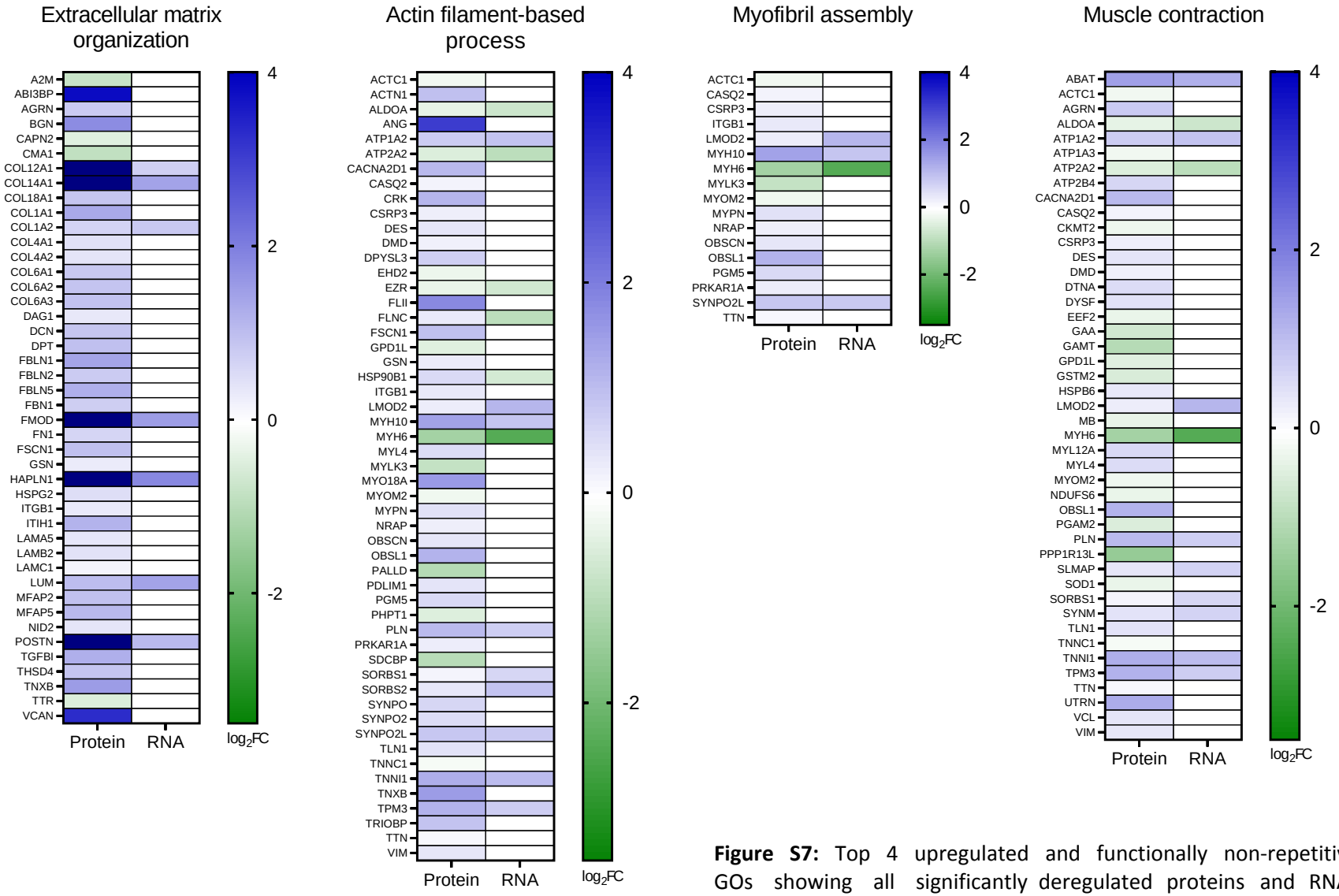

Figure S7: Top 4 upregulated and functionally non-repetitive GOs showing all significantly deregulated proteins and RNAs comparing HCM_{all} with NF_{IVS} annotated to the corresponding GO term. The color gradient indicates the log2 fold change, dark blue beyond the color scale indicates a log2 fold change >4.

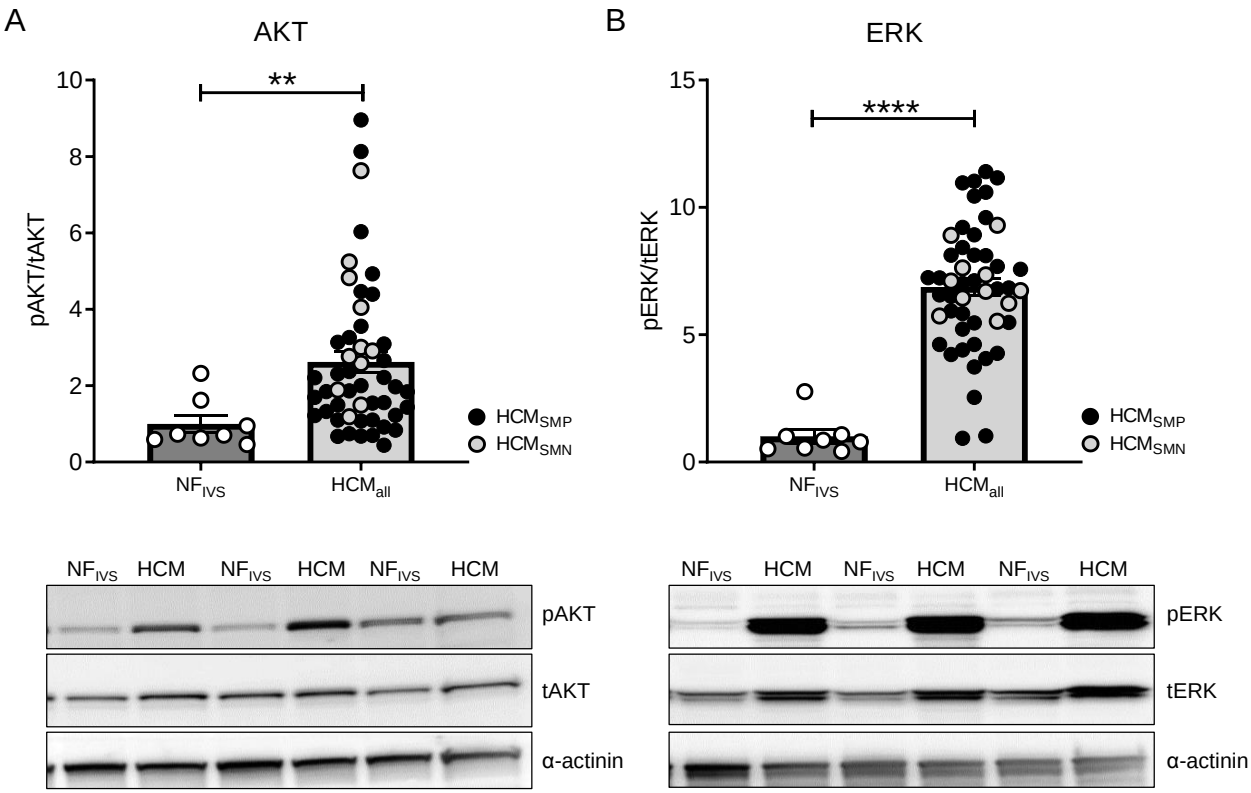

Figure S8: Cardiac hypertrophy markers. Expression (tAKT/tERK) and phosphorylation (pAKT/pERK) of the cardiac hypertrophy markers AKT (A) and ERK (B) with representative western blot images. Alpha-actinin was used as a loading control. Control group was set to 1. n(NF_{IVS})=8, n(HCM_{all})=49; two-tailed Mann-Whitney test, **** p<0.0001, ** p=0.0018.

Figure S9

Downregulated proteins
common for all genotypes

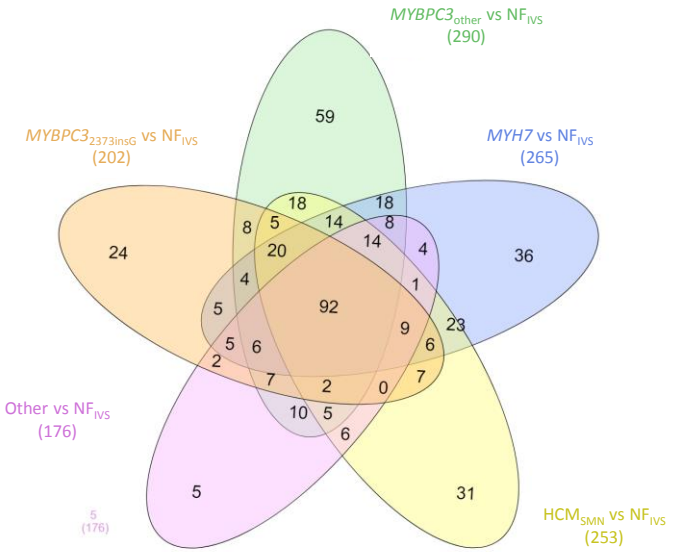

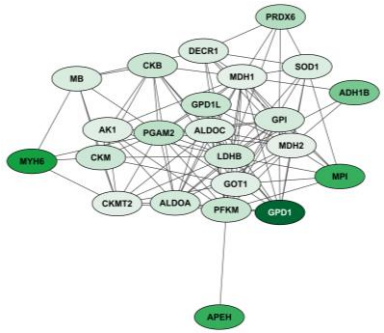

1. NAD metabolic process
(GO: 19674)
23 nodes (p=1.6863E-18)

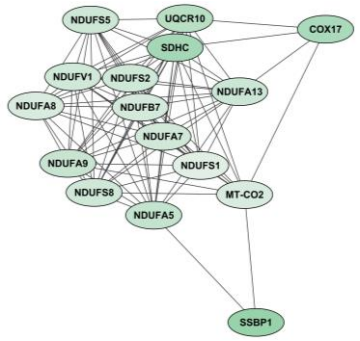

2. Mitochondrial ATP synthesis coupled electron transport
(GO: 42775)
16 nodes (p=2.7090E-31)

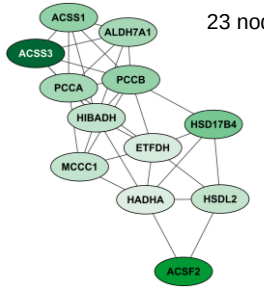

3. Organic acid catabolic process
(GO: 16054)
12 nodes (p=8.8917E-13)

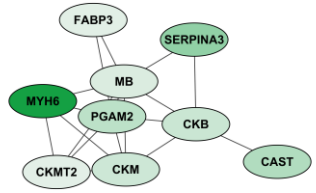

4. Phosphocreatine biosynthetic process
(GO: 46314)
9 nodes (p=3.5124E-10)

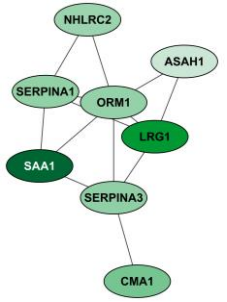

5. Acute-phase response
(GO: 6953)
8 nodes (p=1.4848E-9)

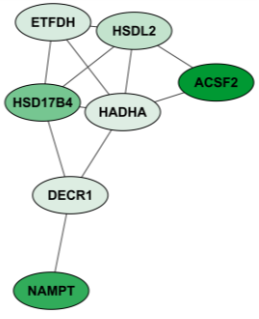

6. Fatty acid beta-oxidation
(GO: 6635)
7 nodes (p=3.2066E-9)

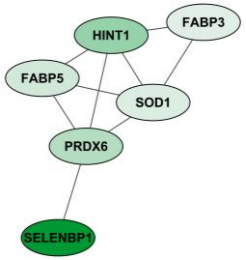

7. Glycerolipid catabolic process
(GO: 46503)
6 nodes (p=4.8674E-7)

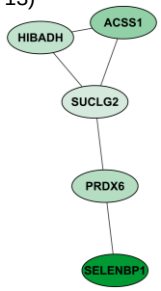

8. Oxidation-reduction process
(GO: 55114)
5 nodes (p=4.6450E-7)

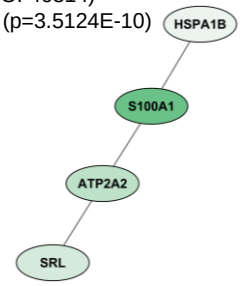

9. Cellular response to heat
(GO: 34605)
4 nodes (p=4.3800E-5)

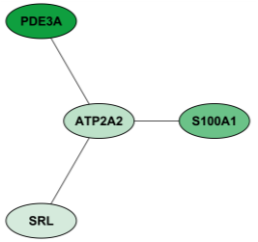

10. Calcium ion transport from cytosol to endoplasmic reticulum
(GO: 1903515)
4 nodes (p=1.6755E-4)

Figure S9: Venn diagram of significantly downregulated proteins of all 5 mutation groups compared to NF_{IVS}. The protein interaction cluster were generated from the overlapping proteins and show downregulated processes, that are common between all groups compared to NF_{IVS}. The color gradient from light to dark indicates an increase in fold change.

Figure S10

Upregulated proteins
common for all genotypes

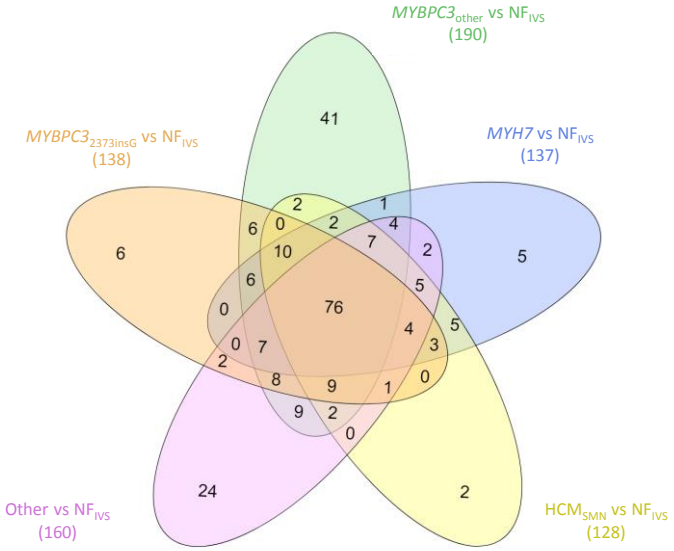

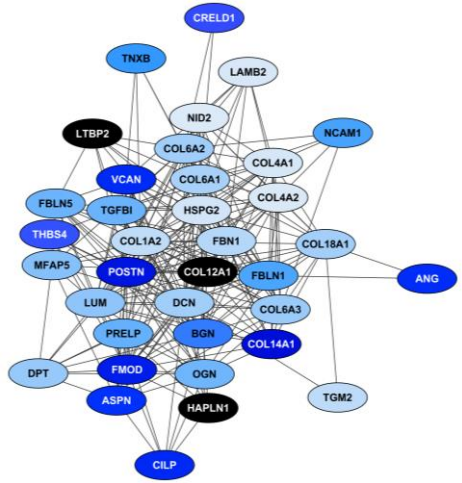

1. Extracellular matrix organization
(GO: 30198)
36 nodes (p=8.1724E-38)

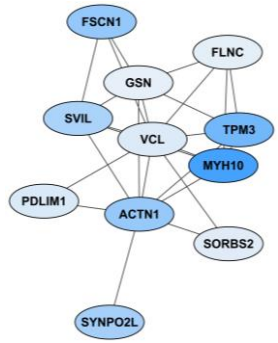

2. Actin cytoskeleton organization
(GO: 30036)
11 nodes (p=4.4911E-11)

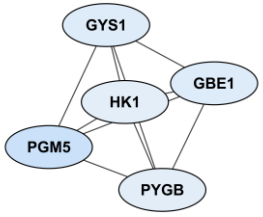

3. Carbohydrate metabolic process
(GO: 5975)
5 nodes (p=1.2470E-8)

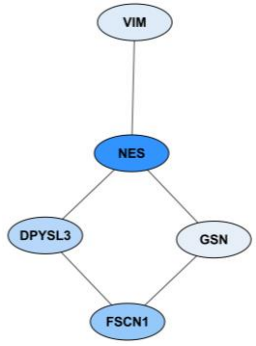

4. Supramolecular fiber organization
(GO: 97435)
5 nodes (p=1.9128E-6)

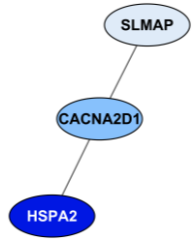

5. Regulation of ion transmembrane transporter activity
(GO: 32412)
3 nodes (p=2.8217E-6)

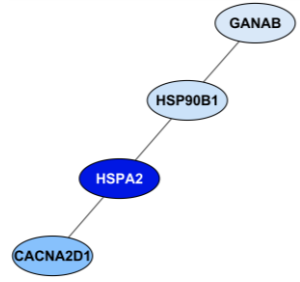

6. Protein folding
(GO: 6457)
4 nodes (p=7.7605E-6)

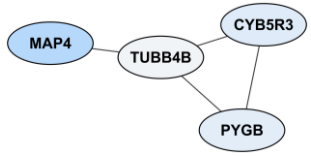

7. Neutrophil degranulation
(GO: 43312)
4 nodes (p=7.5067E-5)

Figure S10: Venn diagram of significantly upregulated proteins of all 5 mutation groups compared to NF_{IVS}. The protein interaction cluster were generated from the overlapping proteins and show upregulated processes, that are common between all groups compared to NF_{IVS}. The color gradient from light to dark indicates an increase in fold change.

Figure S11

Downregulated proteins

HCM_{SMP} vs NF_{IVS}

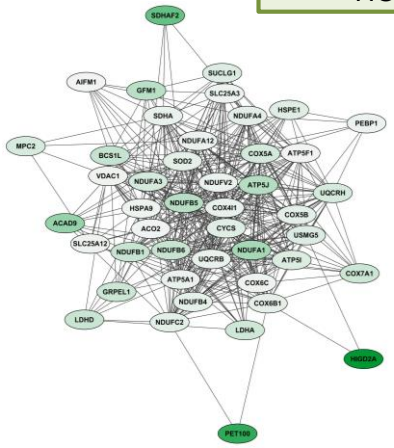

1. Oxidative phosphorylation
(GO: 6119)
45 nodes (p=3.7488E-42)

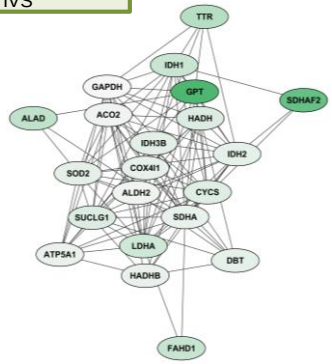

2. Aerobic respiration
(GO: 9060)
21 nodes (p=5.2550E-19)

HCM_{SMN} vs NF_{IVS}

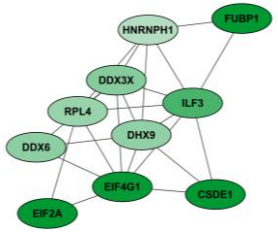

1. Stress granule assembly
(GO: 34063)
10 nodes (p=6.9998E-8)

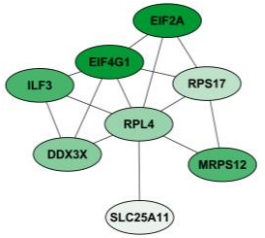

2. Translational initiation
(GO: 6413)
8 nodes (p=1.6065E-9)

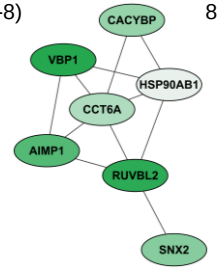

3. Protein folding
(GO: 6457)
7 nodes (p=8.2504E-7)

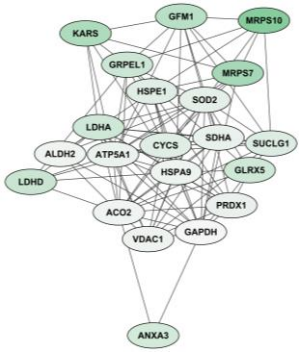

3. Generation of precursor metabolites and energy
(GO: 6091)
21 nodes (p=4.1559E-10)

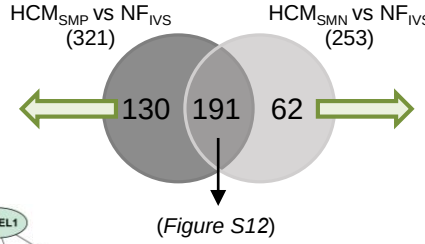

(*Figure S12*)

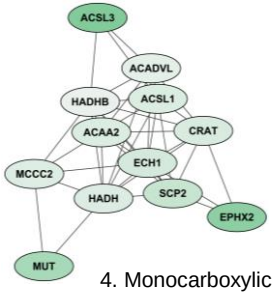

4. Monocarboxylic acid metabolic process
(GO: 32787)
12 nodes (p=3.4967E-19)

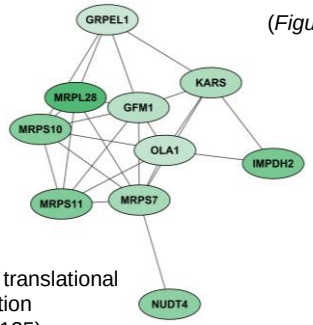

5. Mitochondrial translational elongation
(GO: 70125)
10 nodes (p=5.9619E-10)

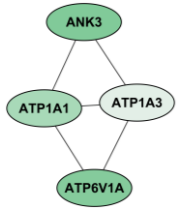

4. Response to glycoside
(GO: 1903416)
4 nodes (p=2.2457E-7)

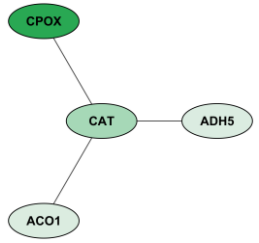

5. Antibiotic metabolic process
(GO: 16999)
4 nodes (p=7.3658E-7)

Figure S11: Differences in downregulated proteins between HCM_{SMP} and HCM_{SMN}. Protein interaction cluster of proteins that are only significantly downregulated for the HCM_{SMP} vs NF_{IVS} or the HCM_{SMN} vs NF_{IVS} comparison were identified and are displayed with the most significant corresponding gene ontology (GO) term. The top 5 protein interaction clusters of downregulated proteins are displayed. The color gradient from light to dark indicates an increase in fold change.

Figure S12

Downregulated proteins
common for HCM_{SMP} and HCM_{SMN} when compared to NF_{IVS}

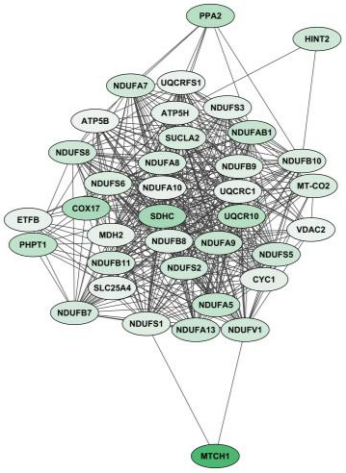

1. Oxidative phosphorylation
(GO: 6119)
37 nodes (p=1.0285E-52)

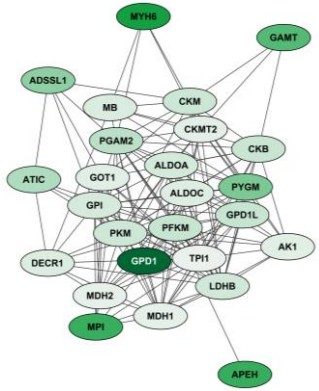

2. NAD metabolic process
(GO: 19674)
26 nodes (p=6.6256E-23)

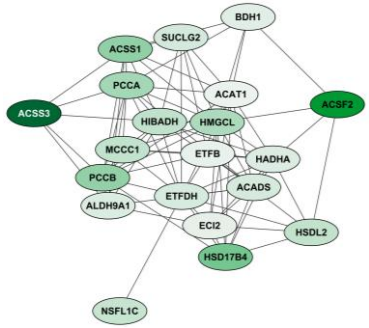

3. Carboxylic acid catabolic process
(GO: 46395)
20 nodes (p=8.5103E-18)

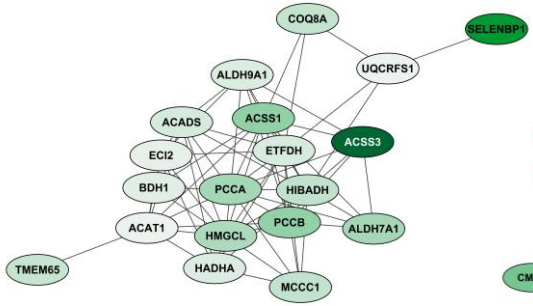

4. Carboxylic acid catabolic process
(GO: 46395)
19 nodes (p=3.6412E-16)

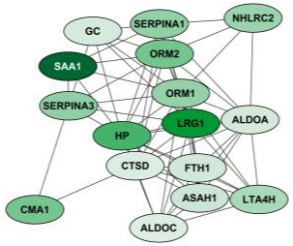

5. Regulated exocytosis
(GO: 45055)
16 nodes (p=1.9023E-16)

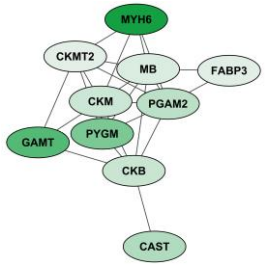

6. Creatine metabolic process
(GO: 6600)
10 nodes (p=1.7159E-12)

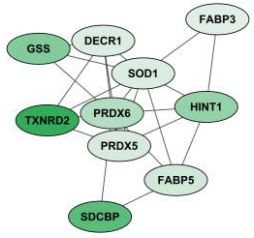

7. Cellular oxidant detoxification
(GO: 98869)
10 nodes (p=1.2808E-7)

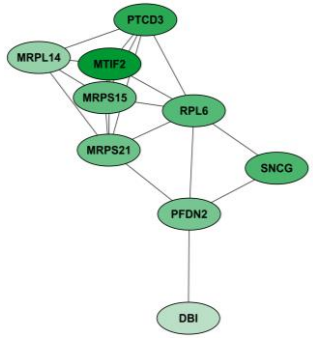

8. Mitochondrial translation
(GO: 32543)
9 nodes (p=1.0811E-9)

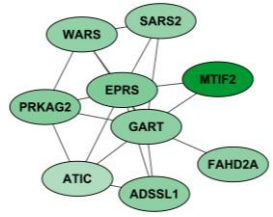

9. Organonitrogen compound
biosynthetic process
(GO: 1901566)
9 nodes (p=1.3873E-9)

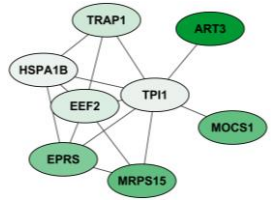

10. Chaperone-mediated
protein folding
(GO: 61077)
8 nodes (p=2.8520E-4)

Figure S12: Protein interaction cluster of all significantly downregulated proteins that are common between HCM_{SMP} compared to NF_{IVS} and HCM_{SMN} compared to NF_{IVS}. The color gradient from light to dark indicates an increase in fold change.

Figure S13

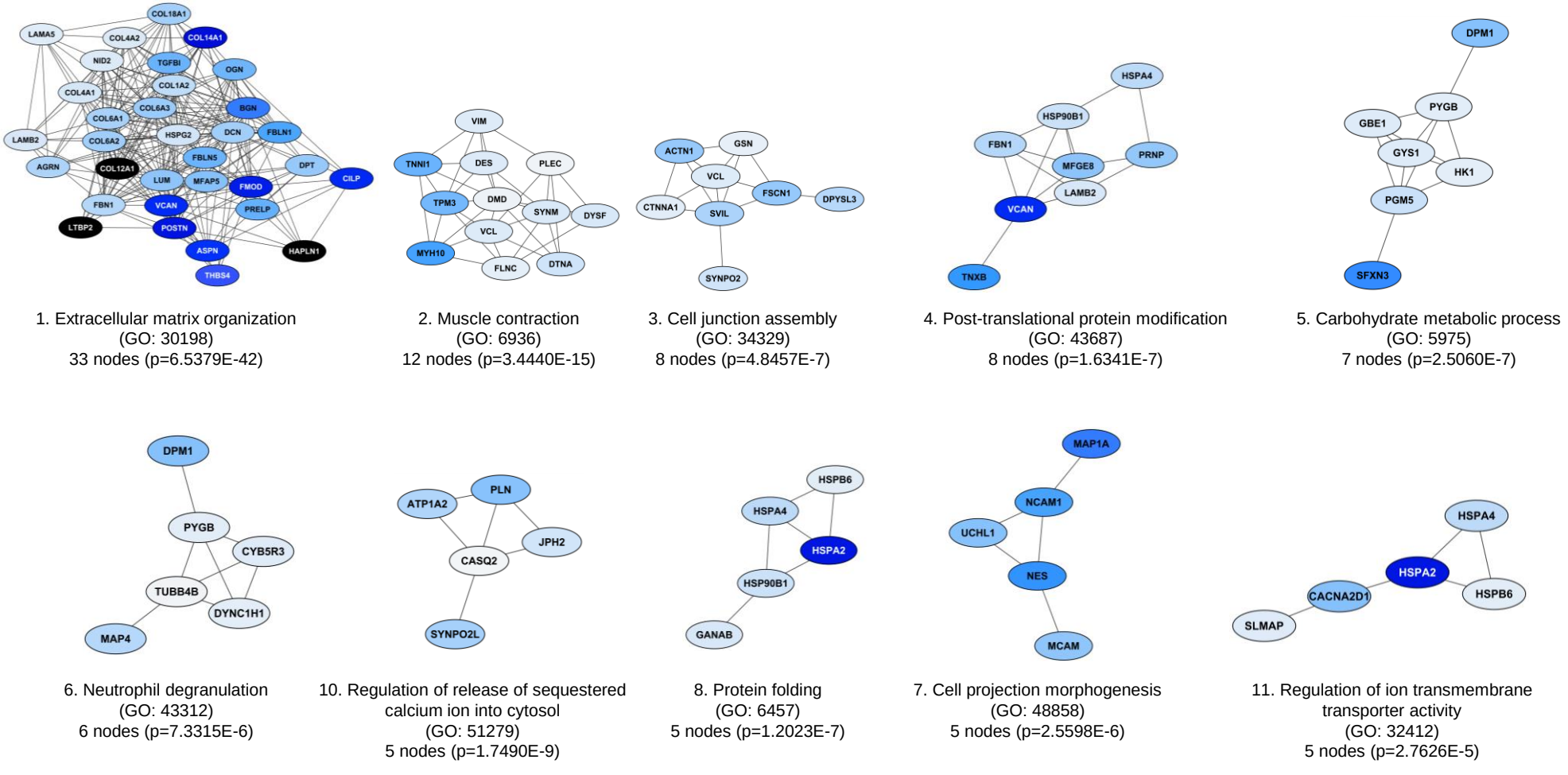

1. Extracellular matrix organization
(GO: 30198)
33 nodes (p=6.5379E-42)

2. Muscle contraction
(GO: 6936)
12 nodes (p=3.4440E-15)

3. Cell junction assembly
(GO: 34329)
8 nodes (p=4.8457E-7)

4. Post-translational protein modification
(GO: 43687)
8 nodes (p=1.6341E-7)

5. Carbohydrate metabolic process
(GO: 5975)
7 nodes (p=2.5060E-7)

6. Neutrophil degranulation
(GO: 43312)
6 nodes (p=7.3315E-6)

10. Regulation of release of sequestered calcium ion into cytosol
(GO: 51279)
5 nodes (p=1.7490E-9)

8. Protein folding
(GO: 6457)
5 nodes (p=1.2023E-7)

7. Cell projection morphogenesis
(GO: 48858)
5 nodes (p=2.5598E-6)

11. Regulation of ion transmembrane transporter activity
(GO: 32412)
5 nodes (p=2.7626E-5)

Figure S13: Protein interaction cluster of all significantly upregulated proteins that are common between HCM$_{SMP}$ compared to NF$_{IVS}$ and HCM$_{SMN}$ compared to NF$_{IVS}$. The color gradient from light to dark indicates an increase in fold change.

Figure S14

A

Upregulated proteins
HCM_{SMP} vs HCM_{SMN}

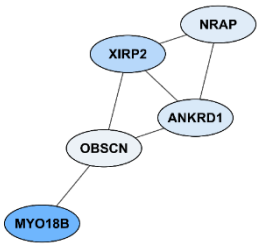

1. Muscle structure development
(GO: 61061)
5 nodes (p=1.2206E-8)

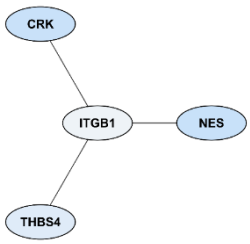

2. Cellular extravasation
(GO: 45123)
4 nodes (p=2.7662E-5)

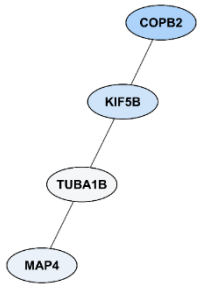

3.1 Establishment of localization in cell
(GO: 51649)
4 nodes (p=1.0527E-4)

3.2 Microtubule-based process
(GO: 7017)
4 nodes (p=1.8282E-4)

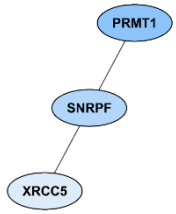

4. Cellular hyperosmotic salinity response
(GO: 71475)
3 nodes (p=5.0260E-4)

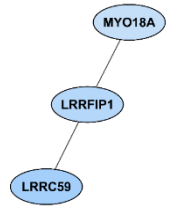

5. Positive regulation of opsonization
(GO: 1903028)
3 nodes (p=1.1170E-4)

B

Downregulated proteins
HCM_{SMP} vs HCM_{SMN}

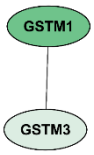

1. Cellular detoxification of nitrogen compound
(GO: 70458)
2 nodes (p=1.8717E-8)

Figure S14: Protein interaction cluster of all significantly upregulated (A) and downregulated (B) proteins resulting from the direct comparison of HCM_{SMP} and HCM_{SMN}. The color gradient from light to dark indicates an increase in fold change.

Figure S15

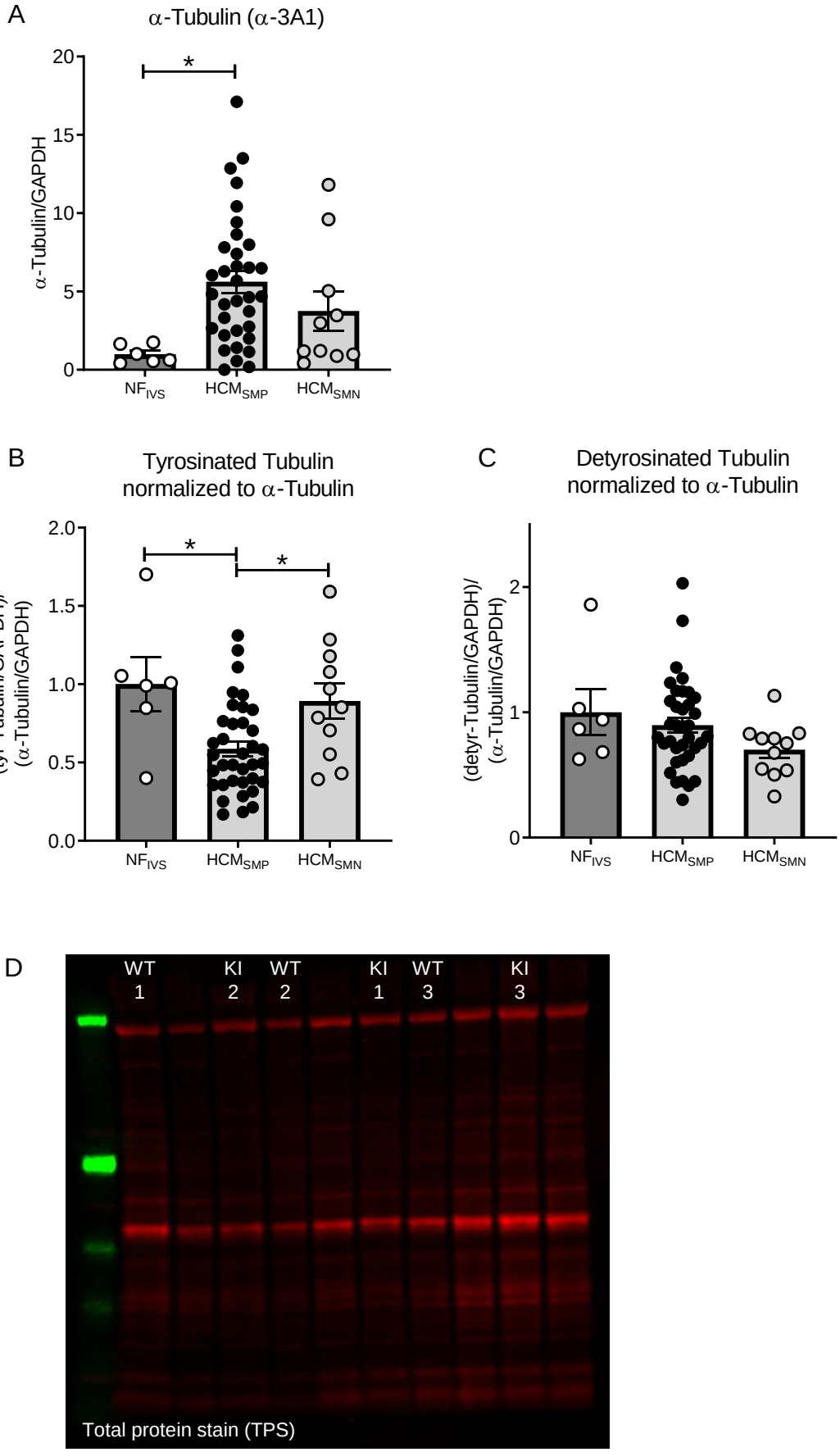
A
α-Tubulin (α-3A1)
α-Tubulin/GAPDH
20
15
10
5
0
*
NF_IVS
HCM_SMP
HCM_SMN
B
Tyrosinated Tubulin
normalized to α-Tubulin
(tyr-Tubulin/GAPDH)/
(α-Tubulin/GAPDH)
2.0
1.5
1.0
0.5
0.0
*
*
NF_IVS
HCM_SMP
HCM_SMN
C
Detyrosinated Tubulin
normalized to α-Tubulin
(detyr-Tubulin/GAPDH)/
(α-Tubulin/GAPDH)
2
1
0
NF_IVS
HCM_SMP
HCM_SMN
D
WT 1
KI 2
WT 2
KI 1
WT 3
KI 3
Total protein stain (TPS)

Figure S15: (A) α-Tubulin (α-3A1) western blot data. Protein levels of α-tubulin with the α-3A1 antibody normalized to GAPDH in tissue of HCM patients. One-way ANOVA with Tukey's multiple comparisons test, * p=0.0257. Average of the control group is set to 1. n(NF_{IVS}/HCM_{SMP}/HCM_{SMN})= 6/34/10. (B) and (C) show the protein levels of tyrosinated and detyrosinated tubulin normalized to total α-Tubulin levels. One-way ANOVA with Tukey's multiple comparisons test, * p<0.05. Average of the control group is set to 1. n(NF_{IVS}/HCM_{SMP}/HCM_{SMN})= 6/36/11. (D) Total protein stain of western blot in Figure 6A that was used as loading control. The lanes labelled with WT 1-3 represent the lanes corresponding to the α-Tubulin bands of the WT mice displayed from left to right, accordingly, KI 1-3 represent the lanes corresponding to the α-Tubulin bands of the *MYBPC3*$_{2373insG}$ mice from left to right.

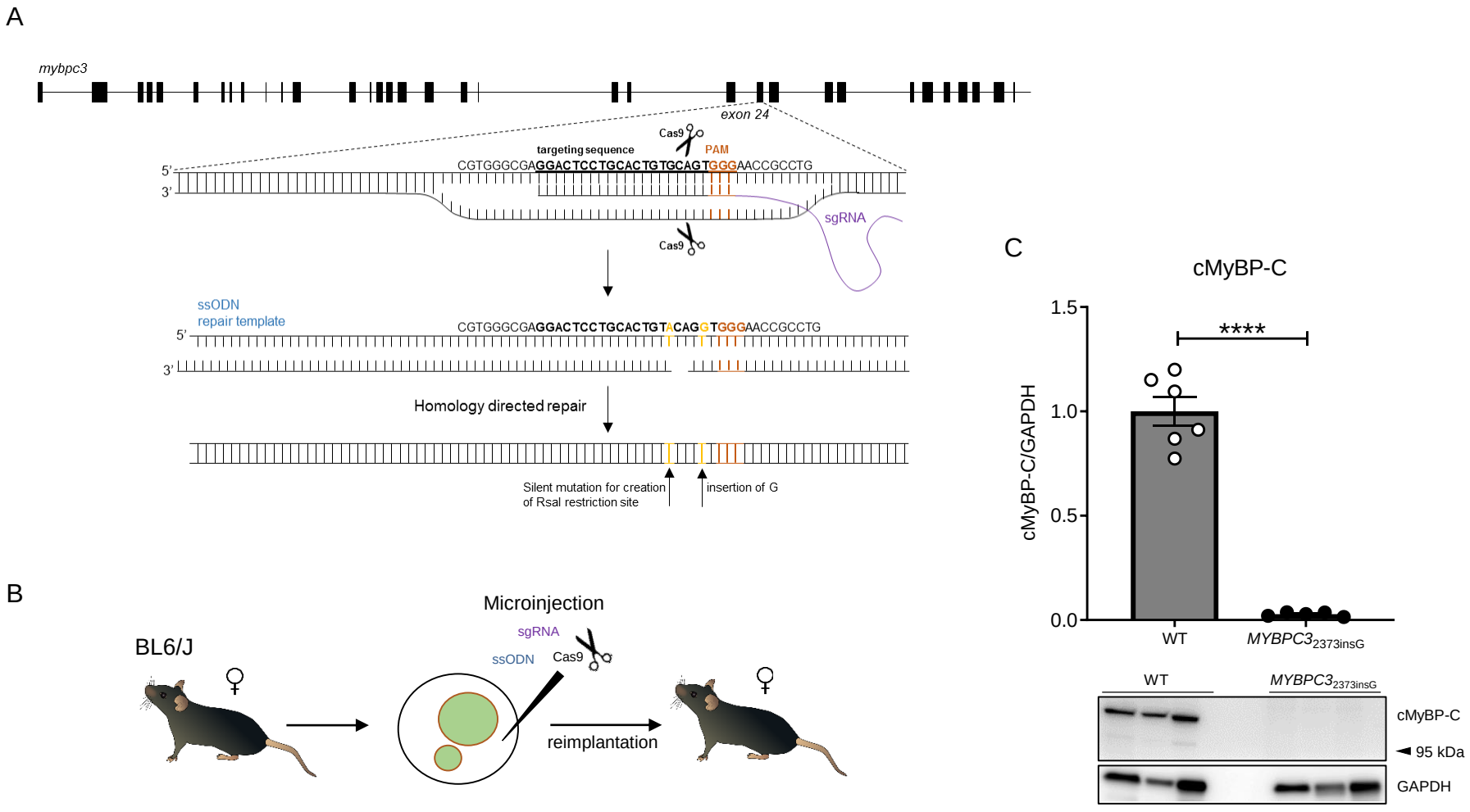

Figure S16: *MYBPC3*$_{2373insG}$ mouse model. (A) Genetic strategy to specifically knock-in the c.2373insG mutation using CRISPR/Cas9. (B) Schematic drawing of the microinjection of all CRISPR/Cas9 components into the zygote. (C) Expression levels of cMyBP-C in the left ventricle of homozygous *MYBPC3*$_{2373insG}$ mice compared to wildtype littermates with no presence of the expected truncated protein of 95kDa. n(WT)=6 (4 females, 2 males; 20-27 weeks) and n(*MYBPC3*$_{2373insG}$)=5 (3 females, 2 males; 22-26 weeks), unpaired two-tailed t-test, **** p<0.0001.

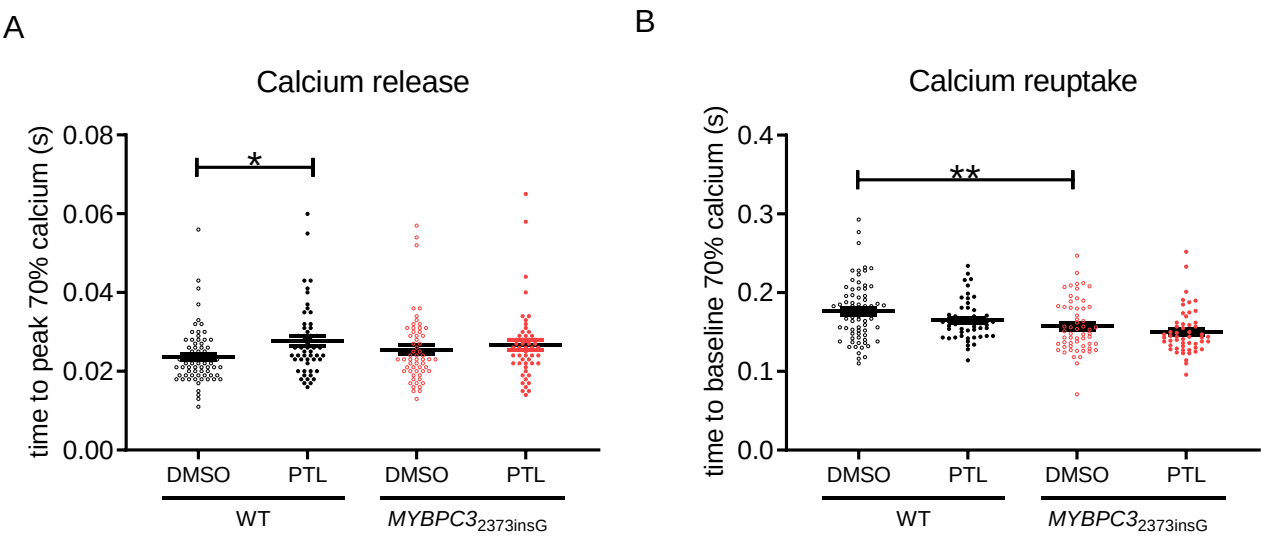

Figure S17: (A) and (B) Calcium kinetics of isolated *MYBPC3*$_{2373insG}$ cardiomyocytes upon inhibition of tubulin detyrosination. (A) displays the effect of PTL on the calcium release parameter time to peak 70% and (B) on the calcium reuptake parameter time to baseline 70%. The dotted line visualizes the WT baseline level. For (A-B) N(WT mice)=2 (2 males, 13-19 weeks) with total n(cells DMSO/PTL)=74/53 and N(*MYBPC3*$_{2373insG}$ mice)=3 (3 males, 13-19 weeks) with total n(cells DMSO/PTL)=58/53. (A) and (B) were analyzed by 2way-ANOVA, ** p=0.0479, ** p=0.0045.